On the Formation of Narrowly Polydispersed PMMA by Surface Initiated Polymerization (SIP) from AIBN-Coated/ Intercalated Clay Nanoparticle Platelets

Xiaowu Fan,† Chuanjun Xia,† and Rigoberto C. Advincula*,‡

Materials Science Program and Department of Chemistry, University of Alabama at Birmingham, Birmingham, Alabama 35294-1240, and Department of Chemistry, University of Houston, Houston, Texas 77204-5003

Received July 26, 2004. In Final Form: December 17, 2004

Various free radical surface initiated polymerization (SIP) conditions were investigated on clay nanoparticles coated with monocationic 2,2′-azobisisobutyronitrile (AIBN) type free radical initiators. Interesting differences in the mechanism of polymer nanocomposite product formation and the role of nanoparticle surface bound AIBN initiators were observed on three types of poly(methyl methacrylate) (PMMA) polymerization conditions: bulk, suspension, and solution. X-ray diffraction (XRD) and differential scanning calorimetry (DSC) measurements confirmed the attachment of the initiator on the clay particles without decomposition of the azo group. XRD and transmission electron microscopy (TEM) showed that a well-dispersed structure was accomplished only by bulk and solution SIP. The suspension SIP product consisted of a partially exfoliated structure as shown by XRD and clay particle aggregate formation as shown by TEM. In general, the molecular weights (MWs) of the surface bound polymers were found to be lower than those of the free polymer. Using the same clay loading and initiator concentrations, we observed that relatively higher MW polymers were obtained from suspension and bulk polymerizations in contrast to solution method. However, the most interesting observation is that the surface bound polymers (on all three conditions) showed much narrower polydispersity compared to that of a typical AIBN type free radical polymerization.

Introduction

Surface initiated polymerization (SIP) involves the growth of polymers from surface bound initiators either on flat surfaces or on particles.[1] This results in the formation of high density polymer brushes where the distance between anchoring points (grafting density) can be smaller than the radius of gyration (R_g) of a free polymer. Essentially, the attachment of initiators to surfaces results in a heterogeneous macrointiator system for polymerization. In this case, the initiation rate, propagation rate, and termination pathways (which determine growth kinetics and mechanism) of a surface bound polymer can be very different from those of a free polymer. For the preparation of polymer nanocomposite materials, this has important consequences. The distribution of the filler/particle and the polymer molecular weight (MW) and polydispersity affect structure−property relationships, that is, thermomechanical, viscoelasticity, and barrier properties.

Recently, there has been intensive interest in preparing poly(methyl methacrylate) (PMMA)−clay nanocomposites because of their improved mechanical properties, thermal stability, flame retardancy, and barrier properties.[2] There are mainly two types of structures for polymer−clay nanocomposites: intercalated and exfoliated.[3] Because of the greater phase homogeneity with the latter, the exfoliated structure is more effective in improving the properties of the polymer, especially at very low clay loading. Different strategies toward PMMA−clay nanocomposites include the following: exfoliation−adsorption, intercalative polymerization, melt intercalation, and template synthesis.[4] The primary route followed typically involves in situ polymerization of the methyl methacrylate (MMA) monomer in the presence of pristine or organically modified clay. The clays were functionalized by various organic cations through ion exchange where the metal ions are replaced by organic cations intercalated between silicate layers. Early studies were focused on mixing MMA monomer with modified/unmodified clay followed by polymerization with azo, peroxide, or persulfate free radical initiators. In situ free radical polymerization of MMA with clay was first demonstrated by Blumstein and co-workers.[5] Other approaches since then have involved: emulsion polymerization,[6,7] suspension polymerizations,[8] melt intercalation,[9] solution polymerization,[10] bulk polymerization,[11] and copolymerizations.[12,13] Amidinium cation-terminated oligoMMA and ammonium salt containing MMA units have been used as organic modifiers of the

* To whom correspondence should be addressed.
† University of Alabama at Birmingham.
‡ University of Houston.

(1) (a) Advincula, R. *J. Dispersion. Sci. Technol.* **2003**, *24*, 343−361. (b) Fan, X.; Xia, C.; Advincula, R. In *Dekker Encyclopedia of Nanoscience and Nanotechnology*; Schwarz, J., Contescu, C., Putyera, K., Eds.; Marcel Dekker: New York, 2004; p 2959.

(2) Zhu, J.; Start, P.; Mauritz, K. A.; Wilkie, C. A. *Polym. Degrad. Stab*. **2002**, *77*, 253.

(3) Burnside, S. D.; Giannelis, E. P. *Chem. Mater.* **1995**, *7*, 1597.

(4) Classification by a review article by: Alexandre, M.; Dubois, P. *Mater. Sci. Eng.* **2000**, *28*, 1.

(5) Blumstein, A. *J. Polym. Sci.* **1965**, *A3*, 2665.

(6) Lee, D. C.; Jang, L. W. *J. Appl. Polym. Sci.* **1996**, *61*, 1117.

(7) Bandyopadhyay, S.; Giannelis, E. P.; Hsieh, A. J. *PMSE Prepr., ACS* **2000**, *82*, 208.

(8) Al-Esaimi, M. M. *J. Appl. Polym. Sci.* **1997**, *66*, 1781.

(9) Tabtiang, A.; Lumlong, S.; Venables, R. A. *Eur. Polym. J.* **2000**, *36*, 2559.

(10) Biasci, L.; Agietto, M.; Ruggeri, G.; Ciardelli, R. *Polymer* **1994**, *35*, 3296.

(11) Okamoto, M.; Morita, S.; Taguchi, H. S.; Kim, Y. H.; Kotaka, T.; Tateyama, H. *Polymer* **2000**, *41*, 3887.

(12) Okamoto, M.; Morita, S.; Kim, Y. H.; Kotaka, T.; Tateyama, H. *Polymer* **2001**, *42*, 1201.

(13) Deitsche, F.; Thomann, Y.; Thomann, R.; Mulhaupt, R. *J. Appl. Polym. Sci.* **2000**, *75*, 396.

10.1021/la048126n CCC: $30.25
Published on Web 02/10/2005

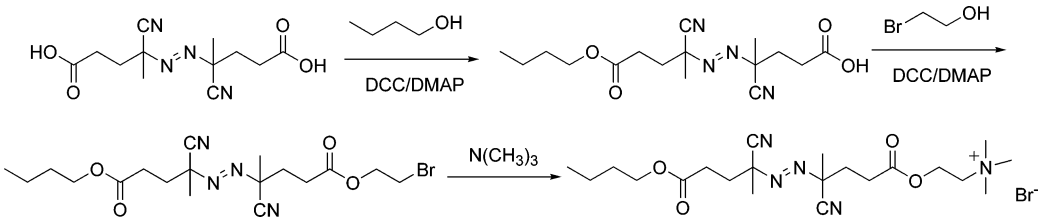

Figure 1. Synthesis scheme of the cationic free radical initiator.

clay, resulting in end-tethered oligomer/polymer chains on clay surfaces after in situ bulk polymerization.[14] The conclusion that surface-attached polymer chains could improve clay particle exfoliation was confirmed by other studies involving intercalating cationic surfactants that contained polymerizable groups.[15,16] Ultimately, it is ideal to have clay particles coated with a polymer shell that is capable of complete compatibilization or miscibility with the host polymer.

In a different approach to all these previously reported systems, we have focused on direct and in situ SIP from partially exfoliated clay nanoparticles. We have also focused on a systematic analysis of the surface bound polymer products. Instead of being initiated in the bulk by the free radical initiator coadded with the monomer or an initiator added to monomer-functionalized clay, initiation is through the activation of initiator derivatives that are *ionically bound* to the clay particle surfaces. The advantage of SIP is based on the assumption that, as the bound polymer chains propagate, any ordered silicate layers could be gradually pushed apart and finally delaminated in the polymer matrix.[15] Furthermore, as compared with the polymerizable surfactant route, SIP can presumably generate more end-tethered polymer chains with greater length, which provide more efficiency in exfoliation. Suter et al. has demonstrated the feasibility of SIP by employing the bicationic azo compound 2,2′-azobis(isobutyramidine hydrochloride) (AIBA) to polymerize styrene from high surface area mica powder.[17] PMMA−clay nanocomposites with exfoliated structure were achieved by Brittain et al. using the same initiator and suspension polymerization.[18] Exfoliated polystyrene−clay nanocomposites with controllable MW were prepared by intercalating a charged living free radical polymerization (LFRP) initiator into montmorillonite.[19] A quasi-living polymerization method, atom transfer radical polymerization (ATRP), has recently been applied to prepare polymer− and copolymer−clay nanocomposites.[20,21] We have previously used a cationic diphenylethylene (DPE) derivative initiator to synthesize polystyrene−clay nanocomposite materials through living anionic surface initiated polymerization (LASIP).[22,23]

Recently, we synthesized a monocationic free radical initiator to graft polymer brush layers of polystyrene from clay particles adsorbed on flat substrates and their surface properties were studied.[24] It should be pointed out that this 2,2′-azobisisobutyronitrile (AIBN) type initiator offers great advantages over the AIBA initiator. First, the positive charge at one chain end is pH-independent. Therefore, the modified clay−initiator structure is insensitive to the surroundings and can tolerate different polymerization conditions. Second, the hydrophobicity of the other end of the initiator can greatly enhance the compatibility between the clay and the organic solution system (Figure 1). This is expected to result in a more homogeneous polymerization system. Moreover, it is interesting to understand the effect of this type of initiator on the MW and polydispersity of surface bound polymers. In this paper, we have focused on the synthesis and characterization of PMMA nanocomposites prepared by coating/intercalating the charged initiator directly into partially exfoliated montmorillonite clay and conducting the SIP by bulk, suspension, and solution conditions. Interesting differences were observed with respect to polymer MW, polydispersity, and polymer-coated clay dispersion properties. The goal is to understand the peculiar conditions and results of a free radical SIP process from clay surface layers compared to free polymers.

Experimental Section

Materials. Montmorillonite clay (commercially Cloisite Na^+, cation exchange capacity (CEC) 92 mequiv/100 g, specific surface area 750 m^2/g) was donated by Southern Clay Products Inc. The deionized water used in all experiments was purified by a Milli-Q Academic system (Millipore Cooperation) with a 0.22 μm Millistack filter at the outlet. MMA (Aldrich) was distilled under reduced pressure at room temperature before polymerization. All other reagents for the initiator synthesis and SIP were commercially available (from Aldrich or Acros) and used without further purification.

Instrumentation. X-ray diffraction (XRD) analysis of initiator-intercalated clay and PMMA−clay composite samples was performed on a Philips X'pert model PW3040-MPD diffractometer with a Cu Kα incident beam of wavelength 0.1543 nm. The Bragg equation was applied to calculate the d spacing of the clay platelets. Differential scanning calorimetry (DSC) was performed on a Mettler model DSC30 instrument with a heating rate of 10 °C/min. Thermal decomposition properties of the azo group of the pure initiator and the intercalated clay were investigated and compared by the STARe software that was integrated in the system. Gel permeation chromatography (GPC) was used to determine the MW (M_n) and the polydispersity index (PDI) of the polymer samples with respect to PMMA standards (21 600−838 000 g/mol). Transmission electron microscopy (TEM) images were obtained on a Philips CM12 microscope operating at 80 kV. Samples were thin-sectioned to ~80 nm by a Riechet Jung UltraCut E microtome.

Initiator Synthesis. The synthesis route of the cationic free radical initiator is shown in Figure 1. Starting with commercially available 4,4′-azobis(4-cyanovaleric acid) (Acros), the carboxylic group at both ends readily undergoes esterification reactions. To prepare a monocationic initiator, the difunctional acid was first treated with 1 equiv of butanol to block one reactive site. Then,

(14) Deitsche, F.; Thomann, R.; Doell, W.; Mulhaupt, R. *PMSE Prepr., ACS* **2000**, *82*, 222.
(15) Zeng, C.; Lee, L. J. *Macromolecules* **2001**, *34*, 4098.
(16) Choi, Y. S.; Choi, M. H.; Wang, K. H.; Kim, S. O.; Kim, Y. K.; Chung, I. J. *Macromolecules* **2001**, *34*, 8978.
(17) Meier, L.; Shelden, R.; Caseri, W.; Suter, U. *Macromolecules* **1994**, *27*, 1637.
(18) Huang, X.; Brittain, W. J. *Macromolecules* **2001**, *34*, 3255.
(19) Weimer, M. W.; Chen, H.; Giannelis, E. P.; Sogah, D. Y. *J. Am. Chem. Soc.* **1999**, *121*, 1615.
(20) Zhao, H.; Shipp, D. A. *Chem. Mater*. **2003**, *15*, 2693.
(21) Bottcher, H.; Hallensleben, M. L.; Nub, S.; Wurm, H.; Bauer, J.; Behrens, P. *J. Mater. Chem.* **2002**, *12*, 1351.
(22) Zhou, Q.; Fan, X.; Xia, C.; Mays, J.; Advincula, R. *Chem. Mater.* **2001**, *13*, 2465.
(23) Fan, X.; Zhou, Q.; Xia, C.; Crsitofoli, W.; Mays, J.; Advincula, R. *Langmuir* **2002**, *18*, 4511.
(24) Fan, X.; Xia, C.; Fulghum, T.; Park, M.-K.; Locklin, J.; Advincula, R. *Langmuir* **2003**, *19*, 916.

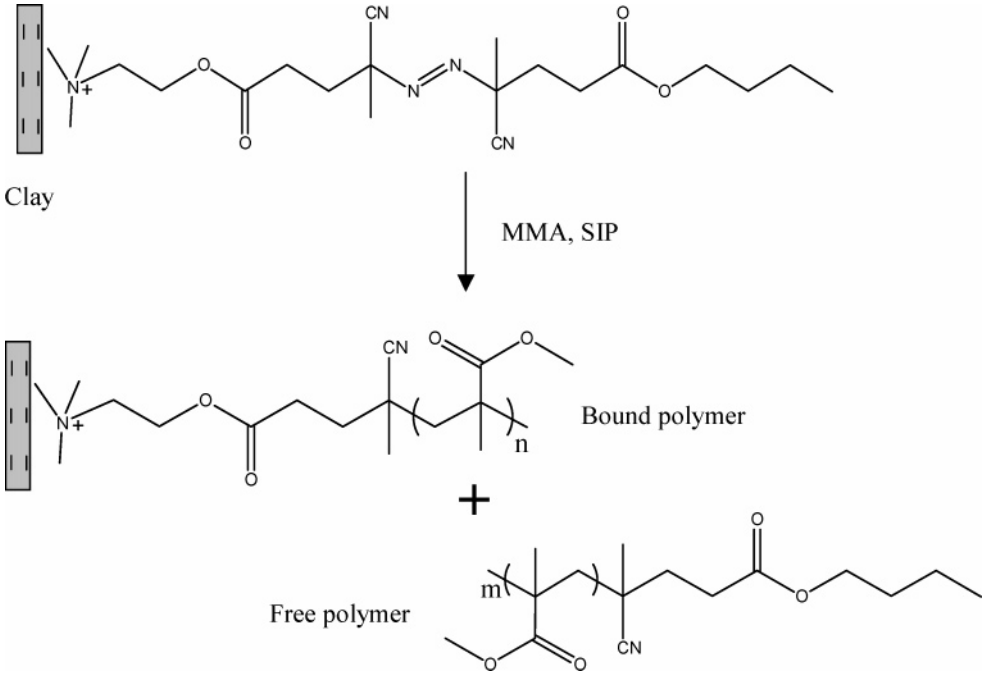

Figure 2. Schematics of the synthesis of PMMA−clay nanocomposites by free radical SIP from clay surfaces.

Table 1. Data Related to the Preparation of the Intercalated Clay

clay used	exact initiator weight	initiator actually added	intercalated clay obtained	yield
1.3 g	0.60 g	0.70 g	1.55 g	87%

the product was esterified with bromoethanol. The bromine-terminated azo initiator was transformed into an organic cation by reacting with anhydrous trimethylamine in tetrahydrofuran. The white precipitate was collected and washed thoroughly with tetrahydrofuran before vacuum drying. The product was characterized by ^{1}H and ^{13}C NMR. Details of the synthesis and characterization have been previously reported.[24]

Intercalated Clay Nanoparticle Preparation. A 1.3 g portion of montmorillonite clay was dispersed in 500 mL of deionized water, and the dispersion was stirred vigorously overnight at room temperature. The clay suspension was then ultrasonicated while stirring for 24 h, and a yellowish, homogeneous clay nanoparticle dispersion was obtained. Previous characterization of nanoparticles prepared using this procedure showed partially exfoliated platelets with an average diameter of 100−300 nm and various thicknesses (lamellae stacking).[23] The initiator was dissolved in deionized water to make a 1.25 wt % solution. By using the CEC value (92 mequiv/100 g) of the Cloisite Na^+ and the MW of the initiator (502.5 g/mol), the exact weight (the weight of the initiator needed to fully replace the Na^+ of the clay) of the initiator was calculated. Accordingly, an excess amount of initiator solution was slowly poured into the clay dispersion while it was being stirred and ultrasonicated. The mixture was stirred and ultrasonicated for another 24 h. The resulting white precipitate was separated by filtration and then redissolved in deionized water. This filtration−dissolution process was repeated 10 times in order to remove the free, unattached initiator. The final product was weighed after drying the precipitates in a vacuum oven at room temperature for 3 days, and the yield percentage was calculated. The yellowish powder product was always stored in a desiccator for further characterization and subsequent SIP. Table 1 summarizes the results of the intercalated clay preparation.

Synthesis of PMMA−Clay Nanocomposites. A schematic illustration of the SIP reaction is shown in Figure 2. For bulk and suspension SIP, 0.071 g of intercalated clay was added to 10 mL of MMA monomer (pure clay loading 0.5 wt % based on MMA). For solution SIP, the same amount of intercalated clay was added to a mixture of 10 mL of MMA monomer and 10 mL of tetrahydrofuran (THF) (HPLC grade, Acros) solvent. All three dispersions were ultrasonicated long enough (usually 6−10 h with active ~30 min cycles and dormant ~5 min intervals) until a homogeneous system was observed. Special care was taken to monitor the temperature to avoid premature decomposition of the AIBN type initiator by adding ice to the sonication water bath. For suspension SIP, the intercalated clay−monomer dispersion was added dropwise to 50 mL of deionized water with vigorous stirring. The three polymerization systems were purged with N_2 flow for 1 h, and the SIPs were carried out at 60 °C for 72 h under N_2 protection. Moreover, a pure PMMA sample (PMMA0) was synthesized as a reference by solution polymerization using recrystallized AIBN initiator under the same conditions. After cooling, an excess amount of methanol was added and the precipitate was filtered and dried in vacuo at room temperature for 3 days. The average yield of the SIP reactions was measured to be ~87%.

Product Separation (Polymer Degrafting Procedure). The crude solid product was dissolved in THF. The yellowish dispersion was centrifuged at 8000 rpm for 10 min. The supernatant liquid that contained free, unattached polymer was separated by decantation. This dissolution−centrifugation−decantation process was repeated three times to remove any physisorbed species. The free PMMA was recovered by adding the decanted solution to excess methanol. For degrafting surface bound polymers, a reverse ion exchange process enabled the detachment of the ionically bound PMMA from the clay surface. After the centrifugation, a solution (1 wt %) of LiBr (Aldrich) in THF was added to the remaining bound PMMA−clay solid and the mixture was stirred and sonicated for 3 h. The resulting dispersion was centrifuged, and the bound polymer solution in THF was obtained by decantation for GPC analysis.

Results and Discussion:

1. Characterizations of the Initiator−Intercalated Clay. The coating and intercalation of the cationic AIBN initiator to clay particles was realized by the cation exchange process. X-ray powder diffraction patterns of pristine clay and intercalated clay are shown in Figure 3. By using the Bragg equation, $n\lambda = 2d \sin\theta$, the d spacing values of the samples were calculated and shown beside each peak. The d spacing value increased from 1.16 nm for original clay to 1.95 nm for intercalated clay, indicating the cationic AIBN initiator molecule was successfully intercalated into the gallery of the partially exfoliated clay particles. Moreover, the increased diffraction intensity

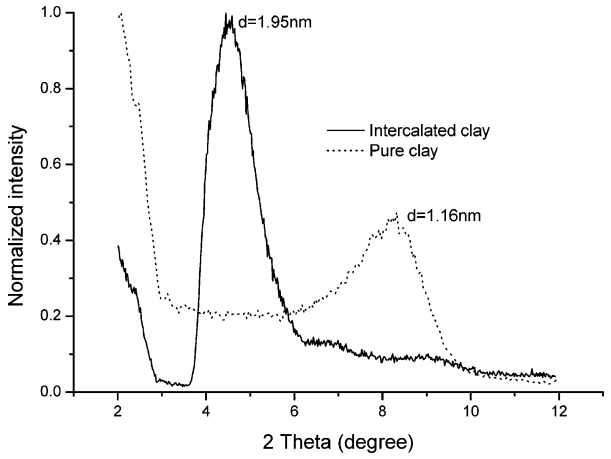

Figure 3. XRD diffractograms of pure clay and intercalated clay.

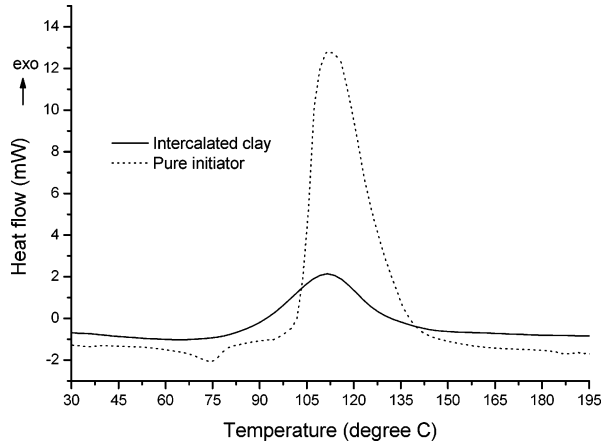

Figure 4. DSC traces of pure initiator and intercalated clay.

indicates a well-ordered swollen structure after intercalation, demonstrating that the layered framework of inorganic clay can accommodate our AIBN type initiator with better structural periodicity. Other than verifying the intercalation procedure, the X-ray data gives no indication of surface coverage on the exposed surface of the clay nanoparticles. However, our previous work on clay particles adsorbed to flat SiO_x surfaces indicates that this process is affine.[24]

The thermal behavior of the pure initiator and the intercalated clay was investigated by DSC. As shown in Figure 4, both samples exhibited a prominent exothermic transition at 80−140 °C, representing the decomposition of the azo group. This further confirms the presence of the initiator on the clay surface/interface. Furthermore, the initiator weight percentage can be calculated by the enthalpy change derived from the DSC traces. The energy released was first calculated by integrating the peak area. The enthalpy/weight ratio was then obtained by dividing the integration by individual sample weight. Similar thermal behaviors were observed and the same quantitative method was applied by Prucker et al.[25,26] and Shirai et al.[27] for nanoparticle materials modified by free radical initiators containing the azo functionality. The results showed 119.7 J g^{-1} for intercalated clay and 376.4 J g^{-1} for the pure initiator. Since there is no enthalpy change for clay in this temperature range, a 31.8 wt % initiator component was determined from the intercalated clay. On the other hand, the ideal initiator weight percentage was calculated to be 28.4 wt % using the CEC data of the montmorillonite clay and the MW of the initiator. One possibility for this difference is that an excessive amount of initiator was added and the free unattached initiators were not totally washed away. Nevertheless, an excess amount of initiator was necessary in order to achieve a complete cation exchange and coating/intercalation process. The basic assumption for the above quantitative method is that the attachment of the initiator molecule does not strongly influence the decomposition behavior of its azo group. This assumption was believed to be reasonable because the decomposition activation energies (E_a) derived from the DSC showed 155 kJ mol^{-1} for the pure initiator and a close value of 148 kJ mol^{-1} for the intercalated one. Prucker and Rühe synthesized similar AIBN type initiators to covalently graft polystyrene layers from spherical silica particles by free radical polymerization.[25] Their surface-attached and pure azochlorosilane initiators demonstrated nearly identical thermal behavior as shown by DSC. They also used DSC and volumetric measurements to quantitatively compare the surface-attached initiators with AIBN initiator in terms of the kinetics (E_a and decomposition rate constant (k_d)) of the azo decomposition.[26] It was concluded that neither the structure modification nor the surface immobilization had a significant effect, because the results showed very similar data for both initiators ($E_a \sim 130$ kJ mol^{-1} and $k_d \sim 7.4-7.5$ s^{-1} for azosilane, $E_a \sim 124-130$ kJ mol^{-1} and $k_d \sim 7.7-7.8$ s^{-1} for AIBN). They believed that the chlorosilane end was decoupled from the azo group by long spacer units in between, which minimized its influence on the decomposition behavior. This explanation can also be applied to the case of our initiator, considering the likeness in their structures. This is further supported by molar enthalpy calculations from DSC measurements. The cationic initiator had a molar enthalpy of 189 kJ $mol^{-1}$and its bromine-terminated precursor (Figure 1) showed a close value of 200 kJ mol^{-1}, indicating the modification by the cationic end did not considerably affect the thermal behavior of the azo group.

In anchoring the initiator to nanoparticle surfaces, it is crucially important to identify and control surface grafting density. In the case of SIP from clay surfaces, it is directly associated with clay loading and the initiator concentration of the SIP reaction. Prucker and Rühe also used DSC data to calculate graft densities of the covalently bound initiators on silica gel particles.[25] The results showed the graft density could be controlled by the initiator concentration in the immobilization reaction and a maximum of 0.8−1.6 molecules/nm^2 could be achieved. However, this methodology is not applicable to our case. The graft density of our ionically bound initiator is determined by the physical properties of the montmorillonite clay: surface charge density, which can be derived from the CEC and specific surface area of the clay. The maximum graft density (complete cation exchange) was calculated to be ~0.74 molecules/nm^2. The actual graft density can also be fine-tuned by varying the ratio of the initiator to a noninitiating cationic surfactant in the cation exchange process.[19] For example, the graft density can be decreased by using a lower initiator/surfactant ratio while keeping the clay content constant. On the other hand, the clay loading can be increased by applying more intercalated clay with a lower initiator/surfactant ratio while keeping the initiator concentration constant. As an alternative method, the actual graft density can also be altered by using other clay products with different CEC

(25) Pruker, O.; Ruhe, J. *Macromolecules* **1998**, *31*, 592.
(26) Pruker, O.; Ruhe, J. *Macromolecules* **1998**, *31*, 602.
(27) Shirai, Y.; Kawatsura, K.; Tsubokawa, N. *Prog. Org. Coat.* **1999**, *36*, 217.

Table 2. MWs and MW Distributions of the Polymers from Different Nanocomposites

sample	initiator/monomer weight ratio	M_n (g/mol)/PDI[a] (free)	M_n (g/mol)/PDI (bound)
PMMA0	N/A[b]	585K/2.35	N/A
Solu-PMMA1	0.0024	292K/2.88	102K/1.46
Susp-PMMA1	0.0024	1744K[c]/2.58	196K/1.28
Bulk-PMMA1	0.0024	1629K[c]/2.67	310K/1.25

[a] Number-average MW (M_n) in grams per mole/polydispersity index (PDI). [b] To obtain comparable MW, the molar ratio of AIBN/MMA was kept the same as that of the three SIPs. [c] The absolute value may not be accurate, as their MWs have exceeded the maximum MW of PMMA standards for GPC.

and surface area values. Clay with a lower CEC can be used to decrease the graft density while keeping the clay loading constant. SIP studies with different clay loadings and initiator concentrations are underway.

Above all, XRD and DSC confirmed the attachment of the initiator molecules, which have replaced all the exchangeable Na^+ ions. Furthermore, our thermogravimetric analysis (TGA) measurements also corroborated this conclusion by demonstrating an initiator content of 30.4 wt % (Supporting Information), which is consistent with the calculated value from DSC results. Besides the above three analytical methods, more comprehensive characterizations on the intercalated clays by infrared (IR) spectroscopy and X-ray photoelectron spectroscopy (XPS) can be found in our recent publications.[28,29]

2. MW and Polydispersity. Successful preparation of the organophilic clay can facilitate free radical SIP because it provides the initiation functionality for polymerization. In addition, it also improves the homogeneity of the intercalated clay−monomer−dispersing agent mixture to achieve an efficient polymerization system. Before making any detailed discussions, it is important to emphasize that there are two kinds of polymers generated under different propagation conditions: *free* polymer and *bound* polymer. In the case of our free radical SIP, the bound polymers grew with their cationic ends tethered to planar clay surfaces.[24,29] They are analogous to polymer brushes grafted from a substrate surface except that these substrates are nanosized and dispersed in monomer/monomer−solvent media. In contrast, the free polymer propagated from the free end of the initiator is not ionically bound to clay surfaces. Free polymers could also originate from residual unattached initiators that were not washed away in the intercalation step or chain transfer from bound chains to free species. Another analogy is that the surface bound polymers were formed from a heterogeneous macrointiator system.

Table 2 summarizes the MW and polydispersity data of the PMMA samples. Figure 5 shows GPC traces illustrating the difference in MW and distribution between free and bound polymers from the three polymerization methods. In general, as shown in Table 2, all three methods, especially suspension and bulk SIP, yielded reasonably high MW products (100−300K), indicating the viability and efficiency of our SIP strategy. However, these values were lower compared to the free polymers (300−1700K) separated from the polymer bound−particle fraction of the nanocomposite. The most logical reason is that the free polymers have higher propagation rates than the surface bound polymers, that is, a typical free radical solution polymerization. Another reason is that clay minerals, especially aluminosilicates, can act as inhibitors for free radical polymerization, where the propagating

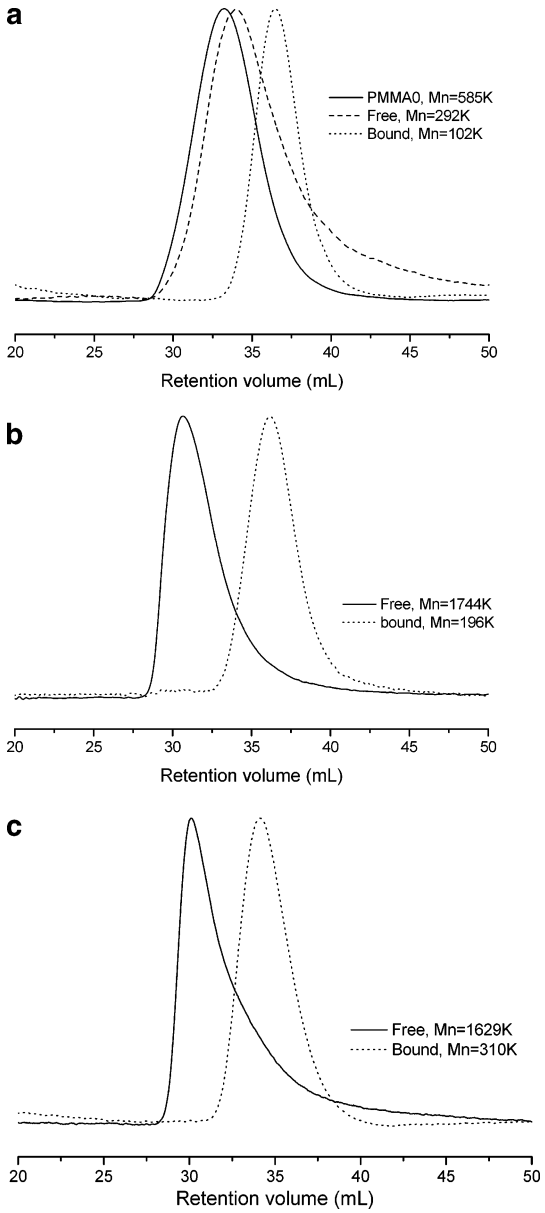

Figure 5. GPC traces of PMMA samples by (a) solution polymerizations, (b) suspension SIP, and (c) bulk SIP.

radicals could be terminated by the adsorption to Lewis acid sites on the clay surface.[30] It should be noted that the ionic adsorption site on clay surfaces is not tight; for example, it can be a few nanometers, depending on the polymorphism.[24]

An important question to ask is how unique is the observed MW difference in the PMMA−clay system compared to other clay nanocomposites. We have previously used similar solution SIP conditions to synthesize polystyrene−clay nanocomposites, and the yields and MWs were significantly lower than those of the PMMA nanocomposites described here.[29] We believe that some of the reasons for this are the following: styrene has a lower propagation rate, a higher termination rate, as well as a larger chain transfer constant compared to MMA.[31] On the other hand, for the efficiency of a heterogeneous monomer−clay−initiator system such as SIP, the com-

(28) Fan, X.; Xia, C.; Advincula, R. *Colloids Surf., A* **2003**, *219*, 75.
(29) Fan, X.; Xia, C.; Advincula, R. *Langmuir* **2003**, *19*, 4381.
(30) Solomon, D. H.; Swift, J. D. *J. Appl. Polym. Sci.* **1967**, *11*, 2567.
(31) Odian G. *Principles of Polymerization*, 2nd ed.; Wiley & Sons: New York, 1981; Chapter 3.

patibility and interaction among the components must be considered. The AIBN derivative initiator contains two highly polar nitrile groups and ester groups. The clay surface is also polar and hydrophilic in nature. MMA monomer possesses methacrylate ester groups that are polar. Thus, compared with the styrene monomer, MMA is of higher polarity and thus more compatible with the clay surface, as previously shown by Blumstein.[32] Similarly, it should also have more compatibility with the polar AIBN type initiator. Other than the polarity factor, the affinity between the ester groups in both initiator and MMA monomer can also contribute to easier monomer diffusion and addition. As a result, we believe that MMA is a more *ideal* monomer compared to styrene for this specific SIP system. Similar differences in terms of MW between polystyrene ($M_n \sim 29-87$K, free polymer) and PMMA ($M_n \sim 106-484$K, free polymer) nanocomposites were also found by Kim and Choi et al. via an emulsion method in which the clay was modified by a polymerizable surfactant containing an acrylamido group.[16,33] Besides the effect on MW, this compatibility issue can also play an important role on the nanocomposite structure of SIP products (will be discussed later). By using different monomers (styrene and MMA) and initiators (AIBN and benzoyl peroxide (BPO)), Zeng and Lee investigated the effect of monomer−initiator−clay compatibility on the final structure of the nanocomposites. Although MW results were not reported, they believed that the better compatibility in the AIBN−MMA−clay system led to higher degrees of dispersion in its nanocomposites than those from the BPO−MMA−clay and AIBN−styrene−clay systems.[15]

Among the three methods, the lowest MW product was observed from solution SIP. It is possible to attribute this to the presence of greater chain transfer effects from the solvent. In addition, its MW is also lower than that of PMMA0 (control) which is prepared without clay (Table 2 and Figure 5a). However, it seemed that these effects did not significantly influence bulk and suspension SIPs, since both produced relatively higher MW free and bound polymers, which is perhaps because they were more prone to the 2-D Trommsdorff effect.[25,26,34] Nevertheless, all were lower compared to their free polymer counterpart. This comparison definitely demonstrates the difference in chain propagation conditions between free and bound polymer. Similar results were previously reported and explained in terms of a slower monomer diffusion and addition to the immobilized radical chains as compared to free ones.[29] Another possible explanation was offered by Tsubokawa et al., who used the free radical SIP method with azo-modified silica and titania particles[35] and glass substrates.[36] It was found that free chains "preferentially proceed" with the polymerization, and they attributed this to the blocking of the surface radicals by the neighboring bound chains especially in the case of the thermal polymerization process.

The most intriguing results though are with the polydispersities of the surface bound polymers. They are quite narrow at ~1.25−1.46 compared to the free polymer values of ~2.67−2.88, which are more typical for an AIBN initiated free radical polymerization process. This is unexpected, given the fact that narrow polydispersities are often observed only with living free radical polymerization methods.[19] Also, previous work by Rühe et al. showed higher polydispersities from SIP on silica gel nanoparticles using a similar type of AIBN initiators.[25,26] We believe that this is one of the first observations of such narrow polydispersities in AIBN-initiated SIP or other nonliving free radical SIP systems for clay nanoparticles.

To explain these results, one must rationalize the effects of chain transfer agents and the various factors affecting the propagation rate and termination mechanisms. A distinctive factor that differentiates the propagation of bound chains from the growth of free ones is the predominance of chain transfer reactions in confined and tethered environments.[24−26] For a surface bound polymer, a chain transfer to monomer or solvent leads to termination. On the contrary, for a free chain, the active center is transferred and the growth of a new free polymer chain begins. Although in the former case a new radical center is also started, it only contributes to the family of free polymers. In other words, chain transfer simply becomes another form of a chain termination mechanism for bound polymers. Minko et al. demonstrated that the termination of bound polymer by chain transfer to free species was truly significant as evidenced by the formation of a substantial amount of free polymer in the bulk even *only* bound radicals were generated upon surface initiation.[37] This not only accounts for the lower MWs of bound polymers but may also explain the intriguing narrower MW distribution differences. Choi et al. observed that the bound polymer chain is significantly shorter than free polymers; that is, the bound radical chains from the polymerizable surfactant they employed only yielded oligomers ($M_n \sim 312$ for polystyrene and $M_n \sim 490$ for PMMA).[16,33] It should be interesting to speculate how the clay−lamellae galleries can influence this phenomenon. In principle, a broadening of polydispersity can be introduced by chain transfer in such a confined environment. However, a controlled diffusion of the monomer, uniform propagation rates, and a similar termination mechanism can off-set this effect. The results indicate a higher efficiency in simultaneous bound chain initiation and propagation. The contribution of the Trommsdorff autoacceleration effect has been previously cited but may not be dominant in this case, because of the clay structure.[25,26]

As shown by their GPC eluograms (Figure 5), all free polymers have small MW "tails". We believe that this is related to the interactions between free polymers and clay surfaces as bound polymer brushes propagating away from clay surfaces. At the early stages of the polymerization, a considerable surface area on clay particles is available (empty).[38] Hence, it is possible that, at the beginning of the polymerization, the fast growing free oligomer/polymer chains are easily terminated by surface Lewis acid sites of the aluminosilicate clay. However, as the polymerization proceeds, the clay particle surfaces are eventually covered by more bound polymers, existing in a *brush* form with more interchain steric repulsion and competition for monomer access. As the distance between anchoring sites becomes much smaller than the radius of gyration (R_g) of a bound polymer ($R_g \sim 10$ nm for PMMA of MW 150K in solution[39]), there is increasing influence of chain transfer effects. For termination, coupling or disproportionation

(32) Blumstein, A. *J. Polym. Sci.* **1965**, *A3*, 2653.
(33) Kim, Y. K.; Choi, Y. S.; Wang, K. H.; Chung, I. J. *Chem. Mater.* **2002**, *14*, 4990.
(34) Minko, S.; Sidorenko, A.; Stamm, M.; Gafijchuk, G.; Senkovsky, V.; Voronov, S. *Macromolecules* **1999**, *32*, 4532.
(35) Tsubokawa, N.; Shirai, Y.; Tsuchida, H.; Handa, S. *J. Polym. Sci., Part A: Polym. Chem.* **1994**, *32*, 2327.
(36) Tsubokawa, N.; Satoh, M. *J. Appl. Polym. Sci.* **1997**, *65*, 2165.
(37) Sidorenko, A.; Minko, S.; Gafijchuk, G.; Voronov, S. *Macromolecules* **1999**, *32*, 4539.
(38) Maximum 0.74 molecule/nm^2 as previously calculated, average distance 1.3 nm between tethering points, assuming hexagonal array and all the initiators have decomposed. The actual density should be lower.

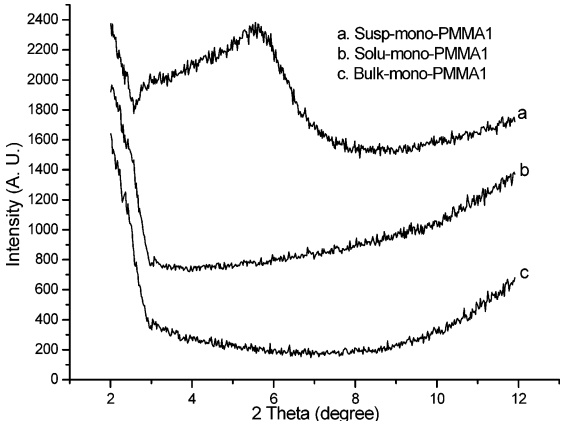

Figure 6. XRD diffractograms of three nanocomposite samples.

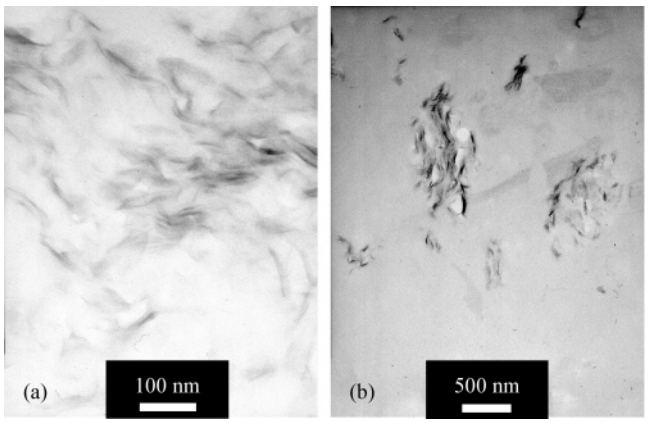

Figure 7. TEM images of (a) Solu-PMMA1 and (b) Susp-PMMA1.

will occur more predominantly among the bound polymers themselves because of their similar restricted degrees of freedom. However, the effects of chain transfer are a major pathway in the termination steps, that is, away from the anchored polymer and toward the monomer, solvent, and free polymer. Some of these possibilities have been previously discussed by Rühe and Prucker, where the rates of initiation, propagation, and termination pathways were affected by the temperature, reaction time, and concentration.[25,26] The important difference is that these observations were detailed from SIP products based on the "open" high surface area of silica gels.

Thus, through initiator intercalation and subsequent SIPs of MMA, we believe that this interesting phenomenon regarding the MW and MW distribution between free and bound polymers is unique for SIP from clay nanoparticle substrates. As revealed by GPC analysis results, this phenomenon needs to be further investigated. Other in situ and kinetic characterization methods and theoretical modeling are needed, which could help in understanding this unique mechanism for improving the properties of final nanocomposite products.

3. Structure of the Nanocomposites. The XRD results show that an exfoliated structure was achieved by solution and bulk SIPs, as their diffractograms in Figure 6 show a featureless pattern. This is confirmed by TEM where an image of disordered clay platelets being well dispersed in polymer matrix was observed (Figure 7a). Again, the homogeneity of the initiator−MMA−clay system during SIP reactions should have contributed to the well-dispersed structure. More importantly, we believe that the dense tethering of the long polymer chains is the critical factor for exfoliation. Tethered polymer chains can promote and preserve the exfoliated morphology by pushing and keeping the silicate layers apart. This key concept has been confirmed by a considerable amount of studies including polymer−clay nanocomposites via the free radical polymerization of other vinyl monomers[40−42] and even other polymerization mechanisms.[43−45] In the case of suspension SIP, compared to those of the pure and intercalated clay, the broad peak suggests that the clay particles have a lesser degree of order but with still moderate short-range periodicities, that is, partially exfoliated structure. This is verified by the TEM observation shown in Figure 7b which exhibits clay aggregates of various sizes in sample Susp-PMMA1. Similar results were found in PMMA−clay nanocomposites prepared from free radical polymerization with the clay modified by a polymerizable surfactant, and a mixed intercalated−exfoliated structure was observed by XRD and TEM.[46] Another study by Yeh et al. also demonstrated the morphology of mixed intercalation−exfoliation in PMMA−clay nanocomposites through in situ free radical polymerization.[47] For suspension polymerization, it is well-known that silicate clays such as montmorillonite can be used as the dispersant to prevent monomer droplets from reagglomerating. In the case of our suspension SIP, the initiator-attached clay not only serves as the suspension stabilizer but also activates the polymerization. Through a similar approach of suspension polymerization of MMA, Huang and Brittain have obtained intercalated and exfoliated structures by alkylammonium- and AIBA-modified clays, respectively.[48] Being significantly different from their initiator as well as experimental procedures, the mixed structure of Susp-PMMA1 probably originated from a portion of amphiphilic intercalated clay that aggregated at the monomer−water interfaces while another portion was exfoliated inside the monomer droplets during suspension SIP. The importance of these properties cannot be underestimated. Recently, we have reported the interesting thermo-oxidative degradation properties of polystyrene−clay nanocomposites prepared by our SIP strategy which showed stability toward antiflammable materials.[49,50]

Conclusions

A monocationic free radical initiator was synthesized and intercalated into partially exfoliated montmorillonite clay nanoparticles. XRD results showed the *d* spacing increased from 1.16 to 1.95 nm after the intercalation. DSC measurements confirmed the attachment of the

(39) Kurata, M.; Tsunashima, Y.; Kwama, M.; Kamada, K. In *Polymer Handbook*, 2nd ed.; Brandrup, J., Immergut, E. H., Eds.; Wiley & Sons: New York, 1975; p IV-38.

(40) Fu, X.; Qutubuddin, S. *Mater. Lett.* **2000**, *42*, 12.
(41) Fu, X.; Qutubuddin, S. *Polymer* **2001**, *42*, 807.
(42) Choi, Y. S.; Wang, K. H.; Xu, M.; Chung, I. J. *Macromolecules* **2002**, *14*, 2936.
(43) Usuki, A.; Kojima, Y.; Kawasumi, M.; Okdada, A.; Fukushima, Y.; Kurauchi, T.; Kamigaito, O. *J. Mater. Res.* **1993**, *8*, 1179.
(44) Messersmith, P. B.; Giannelis, E. P. *J. Polym. Sci., Part A: Polym. Chem.* **1995**, *33*, 1047.
(45) Tyan, H.-L.; Leu, C.-M.; Wei, K.-H. *Chem. Mater.* **2001**, *13*, 222.
(46) Wang, D.; Zhu, J.; Yao, Q.; Wilkie, C. A. *Chem. Mater.* **2002**, *14*, 3837.
(47) Yeh, J.-M.; Liou, S.-J.; Lin, C.-Y.; Cheng, C.-Y.; Chang, Y.-W.; Lee, K.-R. *Chem. Mater.* **2002**, *14*, 154.
(48) Huang, X.; Brittain, W. J. *Polym. Prepr. (Am. Chem. Soc., Div. Polym. Chem.)* **2000**, *41*, 521.
(49) (a) Vyazovkin, S.; Dranca, I.; Fan, X.; Advincula, R. *Macromol. Rapid Commun.* **2004**, *25*, 498. (b) Vyazovkin, S.; Dranca, I.; Fan, X.; Advincula, R. *J. Phys. Chem. B* **2004**, *108*, 11672.
(50) Gilman, J.; Jackson, C.; Morgan, A.; Harris, R., Jr.; Manias, E.; Giannelis, E.; Wuthernow, M.; Hilton, D.; Phillips, S. *Chem. Mater.* **2000**, *12*, 1866.

initiator and demonstrated its azo group decomposition properties were not significantly affected by the intercalation. PMMA−clay nanocomposites were obtained by bulk, solution, and suspension SIPs. XRD and TEM showed that well-dispersed structure was accomplished by bulk and solution SIPs. The structure of the suspension SIP product was partially exfoliated, as shown by a broad peak by XRD and clay particle aggregates by TEM. In general, the MWs of all surface bound polymers for the three methods were lower compared to their corresponding free polymers. Using the same clay loading and initiator concentration, relatively higher MW products were achieved by suspension and bulk polymerizations compared to the solution method. Comparison was made with a similar polystyrene−clay nanocomposite by the SIP method which showed a better homogeneity for the PMMA−clay nanocomposite. More interestingly, the polydispersities of the surface bound polymers were norrower and are unusual for a free radical polymerization based on AIBN initiators. This is attributable to the competing factors between the effects of the clay surface, the propagation rate, the termination pathways, and the chain transfer agents in the different polymerization conditions. Unique in situ characterization methods and theoretical modeling will help elucidate the complete mechanism in these polymer−clay nanoparticle systems. Further studies can be made on other clay loadings and monomer−clay combinations.

Acknowledgment. This project was supported by the Army Research Office (Grant No. DAAD-19-99-1-0106). Montmorillonite clay was generously donated by Southern Clay Product Inc. We appreciate Dr. Yogesh Vohra and Dr. Shane Cetledge, Dr. Sergey Vyazovkin, and Yanxi Zhang at University of Alabama at Birmingham for their help on the XRD and DSC analyses.

Supporting Information Available: Experimental details showing thermogravimetric analysis (TGA) data. This material is available free of charge via the Internet at http://pubs.acs.org.

LA048126N